

---

# Superfluidity vs thermalisation in a nonlinear Floquet system

S. MU<sup>1</sup>, N. MACÉ<sup>3</sup>, J. GONG<sup>1,2</sup>, C. MINIATURA<sup>2,4</sup>, G. LEMARIÉ<sup>2,3,4</sup> and M. ALBERT<sup>5</sup>

<sup>1</sup> *Department of Physics, National University of Singapore, Singapore 117542, Singapore*

<sup>2</sup> *Centre for Quantum Technologies, National University of Singapore, Singapore 117543, Singapore*

<sup>3</sup> *Laboratoire de Physique Théorique, IRSAMC, Université de Toulouse, CNRS, UPS, France*

<sup>4</sup> *MajuLab, International Joint Research Unit UMI 3654, CNRS, Université Côte d'Azur, Sorbonne Université, National University of Singapore, Nanyang Technological University, Singapore*

<sup>5</sup> *Université Côte d'Azur, CNRS, INPHYNI, France*

**Abstract** – We show that superfluidity can be used to prevent thermalisation in Floquet nonlinear systems. Generically, periodic driving boils a many-body system to a featureless infinite temperature state. Fast driving is a known strategy to postpone Floquet heating with a large but always finite boiling time. In contrast, we show the existence, for a nonlinear quantum kicked rotor, of a continuous class of initial states which do not thermalise at all. This absence of thermalisation is associated to the existence of a superflow in momentum space.

**Introduction.** – Thermalisation of isolated quantum systems has been the subject of intensive research during the past decade. In this context, there is an important distinction between ergodicity where the system eventually explores all accessible states, from non-ergodicity. Besides fine-tuned integrable systems whose dynamics is constrained by constants of motion, a seminal example of non-ergodicity is many-body localisation in the presence of strong disorder [1,2]. Other notable ergodicity breaking phenomena include quantum many-body scars and Hilbert space fragmentation [3,4].

A superfluid at zero temperature [5] is another example of conservative system that can evade the fate of thermalisation. As long as its velocity remains smaller than a well defined critical velocity [6], energy transfer from its coherent motion to internal excitations cannot be triggered by its interaction with disorder, hence preventing thermalisation. It is only above this threshold that the system may enter a route toward wave thermalisation [7] or quantum turbulence [8] and eventually reach a statistical equilibrium with an effective temperature. First discovered in liquid Helium [9,10], superfluidity was later shown to be more universal and was observed in various quantum fluids [11–14].

Away from conservative dynamics, time-periodic driving has been used to realize new non-equilibrium phases of matter, e.g. Floquet topological insulator and time crystal [15,16]. However, generic periodically driven interacting systems tend to evolve toward a featureless state

akin to infinite temperature at long times [17–19]. Different mechanisms have been identified to escape this Floquet heating. A first example is many body localisation through strong disorder [20–23]. Another possibility is fast driving, which postpones Floquet heating to exponentially large times and induces a long-lived prethermalization. This mechanism is interesting because it is universal, as it applies to both quantum [26–31] and classical systems [32–36] and does not rely on strong disorder. Nevertheless fast driving does not prevent ultimately the system to boil to infinite temperature.

In this paper, we show that superfluidity can be used in Floquet systems to prevent thermalisation at all times. Using a nonlinear quantum kicked rotor where prethermalization has recently been shown to exist [36], we build a new driving protocol in order to put the system in a superfluid phase and show that the boiling time diverges at the prethermal to superfluid transition.

Our paper is organized as follows. We first introduce the nonlinear kicked rotor model and the new driving protocol allowing for superfluidity to emerge dynamically. We discuss its mapping and difference to conservative superfluids. Superfluidity and heating features are then characterized by gradually increasing the complexity of the model. In the clean case, we perform a Bogoliubov analysis to unveil two important characteristic scales, the analog of sound velocity and healing length. We also describe the Floquet heating instability. We then study the effect of a single impurity. We find two distinct phases, a superfluid

arXiv:2207.06951v1 [cond-mat.quant-gas] 14 Jul 2022

and a turbulent phase, exhibiting dramatically different dynamical behaviours. A superfluid flow is observed up to a critical velocity, given by a Landau criterion [6, 37, 38]. Above that, the system reaches a prethermal phase with a large but finite boiling time. Strikingly, we find that the boiling time diverges at the superfluid-prethermal transition (up to the longest times accessible numerically). Thus, thermalisation is absent in the superfluid phase. Finally, we show that this phenomenology remains valid when taking into account the model in its full complexity, i.e. in the presence of disorder. We describe the statistical properties of the critical velocity with extreme value statistics, in very good agreement with numerical results. Technical details are given in the supplementary material (SM).

**Model.** – The quantum kicked rotor (QKR) we consider is a Floquet system with a very rich phenomenology, from quantum chaos [39, 40] to topological effects [41, 42]. In particular, it displays a phenomenon called dynamical localisation [43], which is analogous to Anderson localisation [44] but in momentum space [45]. This system has been implemented with cold atoms, see e.g. [46–48].

A variant of this model includes mean field Gross-Pitaevskii (GP) interactions [49–51], and has been used to study the breakdown of dynamical localization [49, 52–54], prethermalisation and wave-condensation [36]. This is the model we consider in this work which reads:

$$i\partial_t\psi(p, t) = \mathcal{H}(t)\psi(p, t) + gN_a|\psi(p, t)|^2\psi(p, t), \quad (1)$$

where  $\mathcal{H}(t) = \hat{p}^2/2 - K \cos x \sum_m \delta(t - m)$ , the effective Planck constant has been set to  $\hbar = 1$ ,  $x \in [-\pi, \pi)$  is the angle of the rotor,  $\hat{p} = -i\partial_x$  the associated momentum,  $N_a$  is the number of atoms,  $K$  the kick strength and  $g$  the nonlinear strength. We set a finite-size basis  $|p| \leq N/2$  with periodic boundary conditions in momentum space, the atomic density is equal to unity, i.e.  $N_a = N$ , and normalisation of the state  $\psi$  follows  $\int_{-\pi}^{\pi} |\psi(x, t)|^2 dx / (2\pi) = \sum_p |\psi(p, t)|^2 = 1$ . Denoting  $\psi_n^\pm(\cdot) = \psi(\cdot, t = n \pm 0^+)$ , the dynamics is obtained by iterating the following nonlinear map,

$$\begin{aligned} \psi_{n+1}^-(p) &= e^{-ia_n V(p)} e^{-igN_a |\psi_n^+(p)|^2} \psi_n^+(p), \\ \psi_{n+1}^+(x) &= e^{iK \cos x} \psi_{n+1}^-(x). \end{aligned} \quad (2)$$

Here we have replaced the quasi-random phases induced by the kinetic term  $\hat{p}^2/2$  by an arbitrary potential  $V(p)$ . Indeed, in the kicked rotor, the role of  $p$  and  $x$  is exchanged with respect to standard case, since transport and localisation take place in momentum space. Then, these quasi-random phases can be seen as an effective on-site potential [45], while the kick term  $K \cos x$  plays the role of a kinetic energy. In particular, we will consider  $V(p) = 0$ , the clean case,  $V(p) = W\delta_{p,p_0}$ , a single-impurity, and  $V(p)$  a random uncorrelated potential uniformly distributed between  $[-W/2, W/2]$ , with  $W$  the strength of the potential.

We also consider interactions local in momentum space. The reason for this is twofold: First it corresponds to interactions local in  $x$  for standard systems. Second, it allows to evolve large systems of sizes  $N \sim 10^3$  up to incredibly long times  $t \sim 10^8$ .

Superfluidity will be characterized by a stability analysis of an initial plane-wave in momentum space,  $\psi^0(p) = \frac{1}{\sqrt{N}}e^{-ipx_0}$ , as it flows through a single impurity or disordered potential, in the presence of interactions. Importantly, we do not wish to complicate this analysis by effects induced by a sudden quench of the potential and therefore consider a driving protocol where the potential  $V(p)$  is turned on adiabatically. We have therefore introduced in Eq. (2) a controlling parameter  $a_n$  coupled to  $V(p)$ , whose strength is slowly ramped up as  $a_n = \tanh(n/\tau)$  with  $\tau = 10^3$  unless specified otherwise. We will consider the subsequent dynamics at times  $t \gg \tau$  where the potential is stationary  $a_n V(p) \approx V(p)$ .

At this stage, it is interesting to comment on the analogy of our model with the time evolution of a one dimensional atomic superfluid described by the GP equation in position space,

$$i\hbar\partial_t\phi(x, t) = -\frac{\hbar^2}{2m}\frac{\partial^2}{\partial x^2}\phi(x, t) + g|\phi(x, t)|^2\phi(x, t). \quad (3)$$

In Eq. 3,  $\phi(x, t)$  denotes the macroscopic wave function of a system of identical bosons of mass  $m$  evolving in position space and continuous time. In the clean case  $V(p) = 0$ , our model Eq. (2) can be mapped to the superfluid in real space (3) by mainly inverting position and momentum. However, there are three important differences: (i) In Eq. (3), the second derivative with respect to space, associated with the kinetic energy of the atoms, is quadratic in momentum space and equal to  $p^2/2m$ . In our model (2), the analog term is a cosine term which is only quadratic at small  $x$ . The analogy is therefore restricted to small values of  $x$  with an effective mass given by  $m \equiv 1/K$  (see SM for more details). (ii) Our model (2) is explicitly time-dependent, and we study its dynamics at stroboscopic times. In particular, the periodicity of the non-interacting Hamiltonian  $\mathcal{H}(t)$  gives rise to the existence of Floquet quasi-energy bands which have no equivalence in the static system. As in [36], we will consider a situation where these quasi-energy bands are well separated from each other so that their coupling, due to interactions, is weak. This implies constraints on the parameters of the model which we will discuss later. In this regime, it is also possible to work at low quasi-energy, i.e. at the edge of a quasi-energy band, by considering initial states with sufficiently small  $x_0$ . It is then interesting to investigate whether the physics of a one dimensional superfluid (3) still holds in our system. In particular, this motivates us to transpose the concepts of sound velocity and healing length. (iii) Floquet heating due to the interplay between periodic driving and interaction must be considered in our model. Energy is not conserved, thus the system is gen-

erally expected to evolve toward a featureless state which maximizes the entropy akin to infinite temperature.

**Superfluid properties in the clean case.** – We will now show formally that our model shares important features with usual conservative superfluids described by (3) but in momentum space. In particular, adapting Bogoliubov theory to this Floquet system yields a low energy excitation spectrum that supports the equivalent of sound waves in momentum space. An analog healing length will also be introduced and can be interpreted as a screening length  $\xi$  in momentum space. Along this analysis, a threshold on the kick strength  $K$  is also obtained to avoid fast Floquet heating [55].

In the clean situation, the on site potential is null  $V(p) = 0$  and a plane wave  $\psi^0(p, t) = \frac{1}{\sqrt{N}} e^{-i\phi(t)} e^{-ipx_0}$  is an exact stationary solution under the time evolution in our model if  $\dot{\phi}(t) = -K \cos(x_0) \sum_m \delta(t - m) + g$ . In order to obtain the spectrum of low energy excitations, we perform a linear stability analysis with the ansatz  $\psi(p, t) = \psi^0(p, t)(1 + \delta\psi(p, t))$ . We decompose the perturbation into different modes labeled by  $\theta \in [-\pi, \pi)$ , i.e.  $\delta\psi(p, t) = u(\theta, t)e^{ip\theta} + v^*(\theta, t)e^{-ip\theta}$ . After linearizing Eq. 1, we obtain the time-dependent Bogoliubov-de Gennes equation for the perturbation

$$i\partial_t \begin{pmatrix} u(\theta, t) \\ v(\theta, t) \end{pmatrix} = \mathcal{M}(\theta, t) \begin{pmatrix} u(\theta, t) \\ v(\theta, t) \end{pmatrix}, \quad (4)$$

where  $\mathcal{M}(\theta, t) = \begin{pmatrix} \mathcal{Y}(\theta, t) & g \\ -g & -\mathcal{Y}(\theta, t)^* \end{pmatrix}$  with  $\mathcal{Y}(\theta, t) = -(K \cos(\theta) - K \cos(x_0)) \sum_m \delta(t - m) + g$ . Since the operator  $\mathcal{M}(\theta, t)$  is periodic in time, we consider the one-period evolution operator associated with it, aka the Floquet operator, given by the time-ordered integration  $U(\theta) = \mathcal{T} e^{-i \int_0^1 dt \mathcal{M}(\theta, t)}$ , that is

$$U(\theta) = e^{-i \begin{pmatrix} \lambda & 0 \\ 0 & -\lambda \end{pmatrix}} e^{-i \begin{pmatrix} g & g \\ -g & -g \end{pmatrix}} \quad (5)$$

with  $\lambda = -K \cos(\theta) + K \cos(x_0)$ .

Assuming weak non-linearity strength and small  $\theta$  with  $x_0 = 0$ , i.e.  $g, \lambda \ll 1$ , we can employ the Baker-Campbell-Hausdorff formula [56] to approximate the effective Floquet Hamiltonian for  $U(\theta)$  order by order in both  $g$  and  $\lambda$ , i.e.  $H_F(\theta) = -i \ln U(\theta) \approx H_F^{(1)}(\theta) + H_F^{(2)}(\theta) + \dots$ . At first order in  $g$  and  $\lambda$ , we have

$$H_F^{(1)}(\theta) = \begin{pmatrix} \lambda + g & g \\ -g & -\lambda - g \end{pmatrix}, \quad (6)$$

with eigenvalues at  $x_0 = 0$

$$\omega_{\pm}^{(1)}(\theta) = \pm \sqrt{\frac{K\theta^2}{2} \left( \frac{K\theta^2}{2} + 2g \right)}. \quad (7)$$

Taking  $\omega_+^{(1)}(\theta)$  as the excitation spectrum similar to the Bogoliubov spectrum for time-independent systems, we

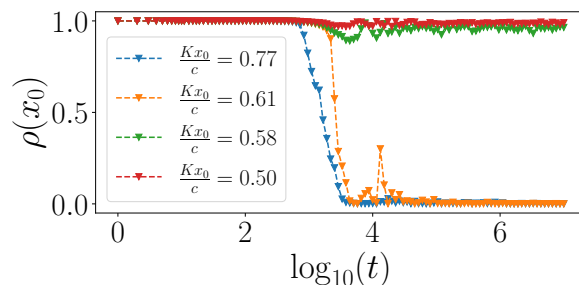


Fig. 1: Density dynamics of several initially prepared modes at different  $x_0$ . The density remain almost unchanged for  $x_0$  below certain critical value, and a drop of the density takes place for  $x_0$  above that critical value. Other parameters are  $K = 1.3, g = 0.1, W\xi/K = 0.41$  and  $N = 1024$ .

can identify a linear dispersion of the low-energy excitations from  $\partial\omega_+^{(1)}/\partial\theta$  with velocity  $c = \sqrt{gK}$ , termed as the sound velocity. Such linear dispersion persists up to  $1/\xi$  with  $\xi = \sqrt{K/g}$  as the healing length in the excitation spectrum.

At this level of approximation, the excitation dynamics of our periodically driven system is identical to that for a time-independent system described by  $H_F^{(1)}(\theta)$ . In particular, Floquet heating is totally absent. It will arise when taking into account higher order terms in the expansion of  $H_F(\theta)$ . In the case of Eq. (5), it is possible to diagonalise exactly  $U(\theta)$  as shown in SM and look for a dynamical instability (eigenvalues of the Floquet operator out of the unit circle). At  $x_0 = 0$  the first unstable mode is  $\theta = \pi$  and appears when  $K + g > \pi/2$  which defines a threshold for Floquet heating. Actually, this criterion has a simple interpretation when considering the relation between the driving frequency  $\Omega = 2\pi/T = 2\pi$  and the effective bandwidth  $E_b$  of our model [27, 36, 57]. The single-particle bandwidth is given by  $E_b = 2K$ , and the correction from non-linearity results in  $E_b = 2(K + g)$  for small  $g$ . An estimate for suppressing the direct inter Floquet band transition is achieved by setting  $E_b = 2(K + g) < \pi$  to avoid fast Floquet heating. In the following, we will set the kick strength  $K < (\pi/2 - g)$  with  $g = 0.1$ .

**Superfluid flow across a single impurity.** – We pursue our investigation of the analogy between the QKR and a conservative superfluid by incorporating an additional ingredient to the model. We now, study the fate of an initial plane wave in the presence of a single impurity  $V(p) = W\delta_{p,p_0}$  of strength  $W$  that is ramped adiabatically in order to avoid the effect of a sudden quench. We show here the possibility of a superflow, namely a flow that propagates without dissipation nor back scattering, in our system even in the presence of the impurity. Again, this superfluid feature shows up in momentum space. In particular, we demonstrate the existence of the analog of a critical velocity for superfluidity.

In traditional superfluids, described by Eq. (3), the na-

ture of the flow interacting with such a single impurity  $W\delta(x)$  is known to be governed by two dimensionless parameters (see [37,38] and SM): The Mach number  $\mathcal{M}$  is the ratio between the velocity of the fluid and the sound velocity which corresponds here to  $\mathcal{M} = Kx_0/c$ . The other parameter is the dimensionless impurity strength which reads here  $\Lambda = W\xi/K$ . In this parameter space, there is a critical line that separates the superfluid phase, at low Mach number, to a turbulent phase. In the superfluid regime, the flow is stationary and therefore no excitation is created from the interaction with the impurity. It therefore lasts forever. Above the critical line, the flow is slowed down by energy transfers from the coherent motion to internal excitations and becomes turbulent.

We will show here that such a critical line also exists in our periodically driven system. Concretely, we initially prepare a coherently populated single mode in position space located at  $x_0$  as a superfluid in momentum space  $\psi(p, t = 0) = \frac{1}{\sqrt{N}}e^{-ipx_0}$ . We then evolve the state stroboscopically under Eq. 2 with  $V(p) = W\delta_{p,p_0}$  for a given  $W$ . The nature of the flow is then established by looking at the evolution of the density in the initial mode  $\rho(x_0, t) = |\psi(x_0, t)|^2$  over a very long time. Figure 1 illustrates our numerical experiment for a given set of parameters.  $\rho(x_0, t \gg \tau)$  shows two different behaviors. Below a critical value of  $x_0$ , denoted as  $x_c$ , the population of the initial plane wave remains very close to unity, meaning that a superflow is established in momentum space. Above this value,  $\rho(x_0, t)$  drops to zero after a certain time, meaning that the initial state is only marginally populated compared to other modes and the superflow is lost.

Then we repeat the simulation with different impurity strength  $W$  to quantitatively find the relation between  $x_c$  and  $W$  or more precisely between  $\mathcal{M}_c$  and  $\Lambda$ . In Fig. 2, we present the critical Mach number  $\mathcal{M}_c$  denoted by the green triangles for the superfluid with the presence of a single-site impurity of different strength  $W$  in our periodically driven system. Our data are compared to the analytical prediction for the critical line  $\Lambda_c(\mathcal{M}_c)$  in a conservative quantum fluid [37,38], with

$$\Lambda_c(\mathcal{M}) = \frac{\sqrt{2}}{4\mathcal{M}} \sqrt{-8\mathcal{M}^4 - 20\mathcal{M}^2 + 1 + (1 + 8\mathcal{M}^2)^{3/2}}. \quad (8)$$

and we observe an excellent agreement.

**Superfluid to prethermal transition.** – Above the critical velocity, the initial plane wave state in momentum space is unstable and the flow turbulent [37,38]. We then expect [36] to enter a prethermal regime which lasts a very long time before Floquet heating boils the system into an infinite temperature state. One of the fundamental characteristics of this prethermal regime is the boiling time  $\tau_{\text{boil}}$ . The question that naturally arises is: is  $\tau_{\text{boil}}$  finite (albeit larger than the observation time considered in figure 1) or infinite in the superfluid phase? In the first case, we would have a meta-stable superfluid state. In this

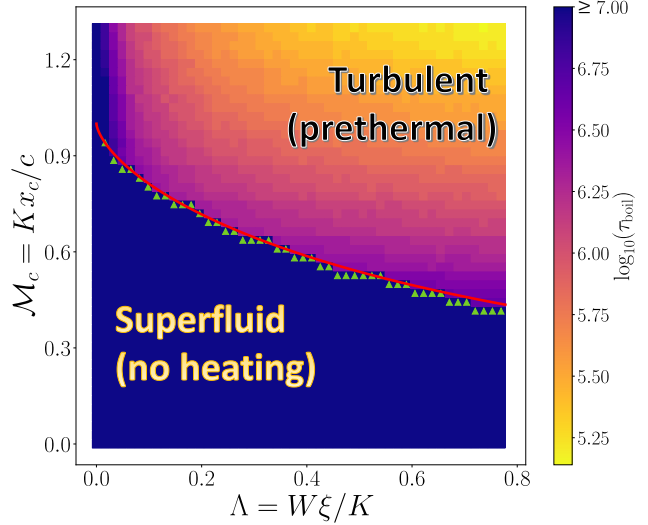


Fig. 2: Phase diagram of the fluid in the presence of a single-site impurity. The critical  $\mathcal{M}_c = Kx_c/c$  denoted by green triangles at different impurity strength  $\Lambda = W\xi/K$  are numerically determined from the density dynamics, and they match very well with the analytical prediction Eq. 8 denoted by the red solid line. Different colors represent the thermalisation time  $\tau_{\text{boil}}$ . Other parameters are  $K = 1.3, g = 0.1$  and  $N = 1024$ .

section, we show the opposite: superfluidity prevents thermalisation at all times in our periodically-driven nonlinear system.

The boiling process induced by Floquet heating is conveniently characterised by the temporal evolution of the variance  $\sigma_x^2(t) = \langle x^2 \rangle - \langle x \rangle^2$  of the angle distribution [36]. In the prethermal regime  $t \ll \tau_{\text{boil}}$ ,  $\sigma_x^2(t)$  shows a plateau while at  $t \gg \tau_{\text{boil}}$  it saturates to the value of a uniform distribution  $\sigma_x^2(t) \approx \pi^2/3$ , a signature of an infinite temperature state. The transition from these two behaviors is sharp and the time at which this happens defines the boiling time. Figures 3(b) and (c) present two examples of simulations in, respectively, the superfluid regime and the turbulent regime. In the first case, the variance remains small and no boiling time could be defined up to the maximal integration time, i.e.  $10^8$  periods. On the contrary, inset (c) demonstrates the existence of a finite boiling time although it is exponentially large.

We now present one of our most important results. In Fig. 3(a), we plot the evolution of  $\tau_{\text{boil}}$  as a function of  $x_0$  at fixed dimensionless impurity strength  $\Lambda = W\xi/K$ . Strikingly, we find that  $\tau_{\text{boil}}$  jumps discontinuously when  $x_0$  crosses the critical  $x_c$  for the superfluid regime previously determined. In the prethermal phase,  $\tau_{\text{boil}}$  is always finite while in the superfluid phase, thermalisation of the system does not take place up to the longest times considered ( $t = 10^8$ ). In Fig. 3(a), the size of the jump of  $\tau_{\text{boil}}$  values for  $x_0$  close to the left or right of  $x_c$  is of nearly two orders of magnitude. This sharp transition at  $x_c$  strongly suggests that the superfluid is immune to Floquet heating.

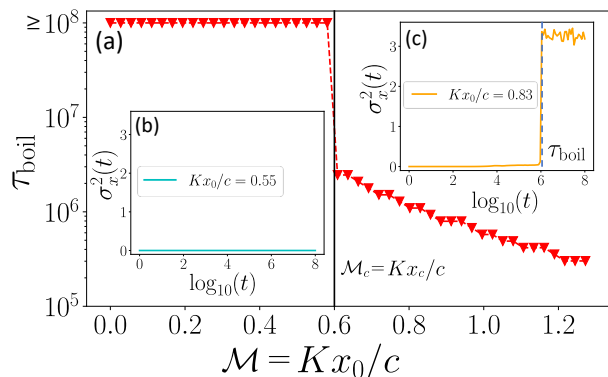


Fig. 3: Variance dynamics of initially prepared modes localized at different  $x_0$  obtained by iterating the nonlinear map in Eq. 2. (a) Scaling of the  $\tau_{\text{boil}}$  vs.  $\mathcal{M} = Kx_0/c$  where  $\mathcal{M}_c$  denoted as the black line is predicted from Eq. 8. (b) The variance for  $x_0 < x_c$  remains small and does not grow (up to  $10^8$  periods). (c) The variance for  $x_0 > x_c$  remains small for an exponentially long time before it saturates and we determine  $\tau_{\text{boil}}$  as indicated by the blue dashed line. Other parameters are  $K = 1.3, g = 0.1, \Lambda = W\xi/K = 0.39$  and  $N = 1024$ .

We also point out that the color map of Fig. 2 represents  $\tau_{\text{boil}}$  as a function of  $\mathcal{M}$  and  $\Lambda$ , as obtained from dynamics up to  $10^7$  periods. Together with our previous phase diagram for turbulence and superfluidity, we find an excellent agreement of the critical  $x_c$  with the points where  $\tau_{\text{boil}}$  diverges. These striking numerical results lead us to conclude that a superfluid below its critical velocity in our periodically driven system is stable, i.e. robust to thermalisation due to either the interaction with the impurity or Floquet heating, or their combined effects.

**Disordered case.** – We now consider our Floquet model Eq.(2) in its full complexity, namely, in the presence of an uncorrelated disordered potential  $V(p) \in [-W/2, W/2]$  with uniform distribution. As expected from the theory of superfluidity [58], the phenomenology observed in the presence of a single impurity remains entirely correct (figures similar to Fig. 2 or Fig.3 have been obtained but are not shown in the manuscript). The only difference is that the critical line in Fig. 2 is now random and depends on the specific configuration of disorder. We therefore discuss here the statistical properties of the critical  $x_c$  as a function of the different parameters.

To compute the critical  $x_c$ , which becomes a random variable now in different disorder realisations, we use arguments based on screening and extreme value statistics [58]. First, we recall that  $\xi$  is the minimal length scale for density fluctuations. Therefore, spatial details of the disorder potential on scales below  $\xi$  cannot be resolved by the system. We therefore renormalise the disorder through a coarse graining procedure over a scale of a few  $\xi$ . Then, we isolate the maximum value of the renormalised disorder and apply criterion (8) to obtain the critical velocity. Using extreme value statistics, it is possible to compute the

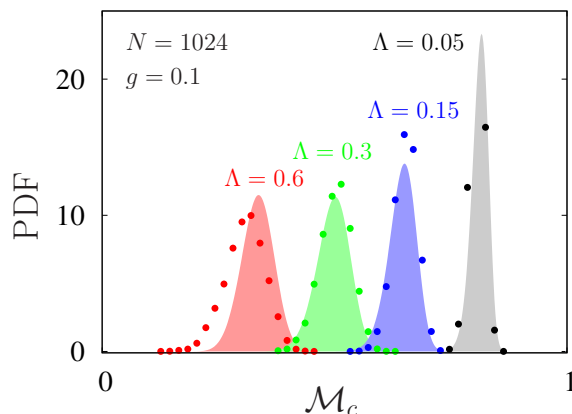


Fig. 4: Probability distribution of the critical  $\mathcal{M}_c = Kx_c/c$  for different disorder strength  $\Lambda = W\xi/K$  at fixed system size  $N = 1024$  and  $g = 0.1$ . Symbols are the histograms extracted from numerical simulations (average over  $10^4$  disorder realisations) whereas shaded curves are the corresponding predictions of the analytical model.

full distribution of the critical velocity as it is explained in SM. This approach gives a rather accurate description of the statistical properties of  $x_c$  as demonstrated below. Our central result is the cumulative distribution of the critical  $\mathcal{M}_c$  which is given by the following formula

$$\Phi_N(\mathcal{M}_c) = 1 - \left[ \frac{1 + \text{erf}\left(\frac{\Lambda_c(\mathcal{M}_c)}{\Lambda_0}\right)}{2} \right]^{\frac{N}{\alpha\xi}} \quad (9)$$

with  $\mathcal{M}_c = Kx_c/c$ ,  $\Lambda_0 = \sqrt{\frac{\alpha\xi}{6}} \left(\frac{W\xi}{K}\right)$  and  $\alpha = 2.78$  (see SM). Then the probability distribution of the critical  $\mathcal{M}_c$  is  $\mathcal{P}_N(\mathcal{M}) = \Phi'_N(\mathcal{M})$ . Note that this simple expression contains nontrivial scaling properties of  $\mathcal{M}_c$  with respect to the system size  $N$ , the disorder strength  $W$ , the kick strength  $K$  and the non-linearity strength  $g$  via  $c$  and  $\xi$ .

In Fig. 4, we present the comparison between numerically extracted histograms of the critical  $\mathcal{M}_c$  and our analytical predictions for different values of the disorder strength  $W$ . The model not only reproduces the typical critical  $\mathcal{M}_c$  and its fluctuations but also the full probability distribution with a remarkable agreement. In order to quantify the typical value of the critical  $\mathcal{M}_c$ , we have computed its median  $\overline{\mathcal{M}_c}$ , defined as  $\Phi_N(\overline{\mathcal{M}_c}) = 1/2$ , as a function of the disorder strength  $W$  and the results are shown in Fig. 5. One can see that it is substantially below the critical velocity predicted by a single impurity but very well captured by the effective disorder computed from extreme value arguments. In addition, we have also checked the scaling with the system size  $N$  (see SM) and  $g$  (data not shown) which give the same level of agreement. Altogether, these results demonstrate that the superfluid to turbulent transition in the disordered case can be understood and accurately described by a coarse graining pro-

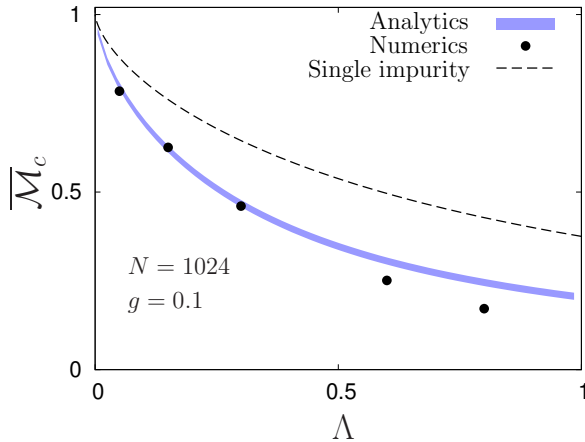


Fig. 5: Median of the critical  $\mathcal{M}_c$  as function of  $\Lambda = W\xi/K$  for  $N = 1024$  and  $g = 0.1$ . The thick line is the extreme value statistics theory whereas the dashed line is the result for a single impurity of strength  $W$ .

cedure. In other words, the single-site impurity case can be taken as an effective description for the case with uniformly distributed disorder at a renormalised strength.

Last, we have also addressed the Floquet heating instability with disorder. We find that the distribution of the critical  $\mathcal{M}_c$  determined above predicts very well the onset of a diverging  $\tau_{\text{boil}}$  (see SM). For a superfluid moving through disorder with initial  $\mathcal{M}_0$  below its renormalised critical  $\mathcal{M}_c$ , thermalisation is not seen to occur under periodic driving.

**Conclusion.** – In this letter, we have shown that superfluidity can be used to prevent thermalisation in non-linear Floquet systems. While fast driving is a well-known mechanism to postpone Floquet heating to exponentially long times, we have demonstrated a model where the boiling time diverges at the superfluid to prethermal transition. This promotes superfluidity as a new mechanism for ergodicity breaking in Floquet systems.

This opens interesting avenues to study Floquet topological superfluids [59] and dynamical phase transitions [60] such as the recently proposed dynamical Berezinskii-Kosterlitz-Thouless phase transition [61].

\*\*\*

We thank P. E. Larré for fruitful discussions. This study has been supported by the French National Research Agency (ANR) under projects COCOA ANR-17-CE30-0024, MANYLOK ANR-18-CE30-0017 and GLADYS ANR-19-CE30-0013, the EUR grant NanoX No. ANR-17-EURE-0009 in the framework of the “Programme des Investissements d’Avenir”, and by the Singapore Ministry of Education Academic Research Fund Tier I (WBS No. R-144-000-437-114). Computational resources were provided by the facilities of Calcul en Midi-Pyrénées (CALMIP) and

the National Supercomputing Centre (NSCC), Singapore. In addition, during the submission process, we became aware of a closely related work [62].

## REFERENCES

- [1] NANDKISHORE R. and HUSE D. A., *Annual Review of Condensed Matter Physics*, **6** (2015) 15.
- [2] ABANIN D. A., ALTMAN E., BLOCH I. and SERBYN M., *Rev. Mod. Phys.*, **91** (2019) 021001.
- [3] SERBYN M., ABANIN D. A. and PAPIĆ Z., *Nature Physics*, **17** (2021) 675.
- [4] MOUDGALYA S., BERNEVIG B. A. and REGNAULT N., *arXiv*, (2021) .
- [5] LEGGETT A. J., *Rev. Mod. Phys.*, **71** (1999) S318.
- [6] LANDAU L. D., *J. Phys. U.S.S.R.*, **5** (1941) 71.
- [7] NAZARENKO S., *Wave turbulence* Vol. 825 (Springer Science & Business Media) 2011.
- [8] VINEN W. F. and NIEMELA J. J., *Journal of Low Temperature Physics*, **128** (2002) 167.
- [9] ALLEN J. F. and MISENER A. D., *Nature*, **141** (1938) 3558.
- [10] KAPITZA P., *Nature*, **141** (1938) 3558.
- [11] OSHEROFF D. D., RICHARDSON R. C. and LEE D. M., *Phys. Rev. Lett.*, **28** (1972) 885.
- [12] RAMAN C., KÖHL M., ONOFRIO R., DURFEE D. S., KUKLEWICZ C. E., HADZIBABIC Z. and KETTERLE W., *Phys. Rev. Lett.*, **83** (1999) 2502.
- [13] AMO A., LEFRÈRE J., PIGEON S., ADRADOS C., CIUTI C., CARUSOTTO I., HOUDRÉ R., GIACOBINO E. and BRAMATI A., *Nature Physics*, **5** (2009) 805.
- [14] MICHEL C. *et al.*, *Nat. Commun.*, **9** (2018) 2108.
- [15] WEITENBERG C. and SIMONET J., *Nature Physics*, **17** (2021) 1342.
- [16] ELSE D. V., BAUER B. and NAYAK C., *Phys. Rev. X*, **7** (2017) 011026.
- [17] D’ALESSIO L. and RIGOL M., *Phys. Rev. X*, **4** (2014) 041048.
- [18] PONTE P., CHANDRAN A., PAPIĆ Z. and ABANIN D. A., *Annals of Physics*, **353** (2015) 196 .
- [19] REITTER M., NÄGER J., WINTERSPERGER K., STRÄTER C., BLOCH I., ECKARDT A. and SCHNEIDER U., *Phys. Rev. Lett.*, **119** (2017) 200402.
- [20] PONTE P., PAPIĆ Z., HUVENEERS F. M. C. and ABANIN D. A., *Phys. Rev. Lett.*, **114** (2015) 140401.
- [21] LAZARIDES A., DAS A. and MOESSNER R., *Phys. Rev. Lett.*, **115** (2015) 030402.
- [22] KHEMANI V., LAZARIDES A., MOESSNER R. and SONDHI S. L., *Phys. Rev. Lett.*, **116** (2016) 250401.
- [23] ELSE D. V., BAUER B. and NAYAK C., *Phys. Rev. Lett.*, **117** (2016) 090402.
- [24] SEETHARAM K. I., BARDYN C.-E., LINDNER N. H., RUDNER M. S. and REFAEL G., *Phys. Rev. X*, **5** (2015) 041050.
- [25] IADECOLA T., NEUPERT T. and CHAMON C., *Phys. Rev. B*, **91** (2015) 235133.
- [26] ABANIN D. A., DE ROECK W. and HUVENEERS F. M. C., *Phys. Rev. Lett.*, **115** (2015) 256803.
- [27] BUKOV M., GOPALAKRISHNAN S., KNAP M. and DEMLER E., *Phys. Rev. Lett.*, **115** (2015) 205301.
- [28] MORI T., KUWAHARA T. and SAITO K., *Phys. Rev. Lett.*, **116** (2016) 120401.

- [29] MALLAYYA K., RIGOL M. and DE ROECK W., *Phys. Rev. X*, **9** (2019) 021027.
- [30] RUBIO-ABADAL A., IPPOLITI M., HOLLERITH S., WEI D., RUI J., SONDHI S. L., KHEMANI V., GROSS C. and BLOCH I., *Phys. Rev. X*, **10** (2020) 021044.
- [31] PENG P., YIN C., HUANG X., RAMANATHAN C. and CAPPELLARO P., *Nature Physics*, **17** (2021) 444.
- [32] MORI T., *Phys. Rev. B*, **98** (2018) 104303.
- [33] RAJAK A., DANA I. and DALLA TORRE E. G., *Phys. Rev. B*, **100** (2019) 100302.
- [34] HOWELL O., WEINBERG P., SELS D., POLKOVNIKOV A. and BUKOV M., *Phys. Rev. Lett.*, **122** (2019) 010602.
- [35] HODSON W. and JARZYNSKI C., *Phys. Rev. Research*, **3** (2021) 013219.
- [36] HALDAR P., MU S., GEORGEOT B., GONG J., MINIATURA C. and LEMARIÉ G., *arXiv e-prints*, (2021) arXiv:2109.14347.
- [37] HAKIM V., *Phys. Rev. E*, **55** (1997) 2835.
- [38] LEBOEUF P. and PAVLOFF N., *Phys. Rev. A*, **64** (2001) 033602.
- [39] FELIX M. IZRAILEV, *Phys. Rep.*, **196** (1990) 299
- [40] FRITZ HAAKE, *Quantum Signatures of Chaos*, **Springer-Verlag, Berlin, Heidelberg** (2006)
- [41] DAHLHAUS J. P., EDGE J. M., TWORZYDŁO J. and BEENAKKER C. W., *Phys. Rev. B*, **84** (2011) 115133.
- [42] Floquet topological semimetal phases of an extended kicked Harper model RADITYA WEDA BOMANTARA, GUDAPATI NARESH RAGHAVA, LONGWEN ZHOU, AND JIANGBIN GONG, *Phys. Rev. E*, **93** (2016) 022209.
- [43] GIULIO CASATI, BV CHIRIKOV, FM IZRAELEV, AND JOSEPH FORD, *Stochastic behavior in classical and quantum Hamiltonian systems*, **Springer** (1979) 334
- [44] ELIHU ABRAHAMS, ED., *50 Years of Anderson Localization*, **World Scientific** (2010)
- [45] D. R. GREMPEL, R. E. PRANGE, AND SHMUEL FISHMAN, *Phys. Rev. A*, **29** (1984) 1639
- [46] F.L. MOORE, J.C. ROBINSON, C.F. BHARUCHA, P.E. WILLIAMS, AND M.G. RAIZEN, *Phys. Rev. Lett.*, **73** (1994) 2974
- [47] J. CHABÉ, G. LEMARIÉ, B. GRÉMAUD, D. DELANDE, P. SZRIFTGISER, AND J.C. GARREAU, *Phys. Rev. Lett.*, **101** (2008) 255702
- [48] GABRIEL LEMARIÉ, JULIEN CHABÉ, PASCAL SZRIFTGISER, JEAN CLAUDE GARREAU, BENOÎT GRÉMAUD, AND DOMINIQUE DELANDE, *Phys. Rev. A*, **80** (2009) 043626.
- [49] SHEPELYANSKY D., *Phys. Rev. Lett.*, **70** (1993) 1787.
- [50] GLIGORIĆ G., BODYFELT J. D. and FLACH S., *EPL (Europhysics Letters)*, **96** (2011) 30004.
- [51] SAMUEL LELLOUCH, ADAM RANÇON, STEPHAN DE BIÈVRE, DOMINIQUE DELANDE, AND JEAN CLAUDE GARREAU, *Phys. Rev. A*, **101** (2020) 043624.
- [52] NICOLAS CHERRORRET, BENOÎT VERMERSCH, JEAN CLAUDE GARREAU, AND DOMINIQUE DELANDE, *Phys. Rev. Lett.*, **112** (2014) 170603.
- [53] ALEC CAO, ROSHAN SAJJAD, HECTOR MAS, ETHAN Q. SIMMONS, JEREMY L. TANLIMCO, EBER NOLASCO-MARTINEZ, TOSHIHIKO SHIMASAKI, H. ESAT KONDAKCI, VICTOR GALITSKI, DAVID M. WELD, *arXiv*, (2021) 2106.09698.
- [54] JUN HUI SEE TOH, KATHERINE C. MCCORMICK, XINXIN TANG, YING SU, XI-WANG LUO, CHUANWEI ZHANG, SUBHADEEP GUPTA, *arXiv*, (2021) 2106.13773.
- [55] LELLOUCH S., BUKOV M., DEMLER E. and GOLDMAN N., *Phys. Rev. X*, **7** (2017) 021015.
- [56] ACHILLES R. and BONFIGLIOLI A., *Archive for History of Exact Sciences*, **66** (2012) 295.
- [57] MAXIMILIAN GENSKE and ACHIM ROSCH, *Phys. Rev. A*, **92** (2015) 062108.
- [58] ALBERT M., PAUL T., PAVLOFF N. and LEBOEUF P., *Phys. Rev. A*, **82** (2010) 011602.
- [59] MATTHEW S. FOSTER, VICTOR GURARIE, MAXIM DZERO, AND EMIL A. YUZBASHYAN,, *Phys. Rev. Lett.*, **113** (2014) 076403.
- [60] MARKUS HEYL,, *Rep. Prog. Phys.*, **81** (2018) 054001.
- [61] T. SCOQUART, D. DELANDE, N. CHERRORRET, *arXiv*, (2022) 2205.07551.
- [62] M. MARTINEZ, P. E. LARRÉ, D. DELANDE, N. CHERRORRET, *arXiv*, (2022) 2207.05037.

# Supplementary material for "Superfluidity vs thermalisation in a nonlinear Floquet system"

S. MU<sup>1</sup>, N. MACÉ<sup>3</sup>, J. GONG<sup>1,2</sup>, C. MINIATURA<sup>2,4</sup>, G. LEMARIÉ<sup>2,3,4</sup> and M. ALBERT<sup>5</sup>

<sup>1</sup> Department of Physics, National University of Singapore, Singapore 117542, Singapore

<sup>2</sup> Centre for Quantum Technologies, National University of Singapore, Singapore 117543, Singapore

<sup>3</sup> Laboratoire de Physique Théorique, IRSAMC, Université de Toulouse, CNRS, UPS, France

<sup>4</sup> MajuLab, International Joint Research Unit UMI 3654, CNRS, Université Côte d'Azur, Sorbonne Université, National University of Singapore, Nanyang Technological University, Singapore

<sup>5</sup> Université Côte d'Azur, CNRS, INPHYNI, France

**Abstract** –\*\*\* Missing author \*\*\*

This supplementary contains the following material arranged by sections:

1. We present the mapping between the superfluid in our periodically kicked model and that described by the Gross-Pitaevskii equation in position space.
2. We provide details of the derivation of the Bogoliubov expansion in our model without impurities.
3. We provide details of the derivation of the effective impurity strength in the disordered periodically kicked rotor.

## Mapping to the Gross-Pitaevskii equation. –

We explain here in details the correspondance between our model and the one of a one dimensional superfluid described by the Gross-Pitaevskii equation in the presence of a single impurity

$$i\hbar\partial_t\phi(x,t) = -\frac{\hbar^2}{2m}\frac{\partial^2}{\partial x^2}\phi(x,t) + g|\phi(x,t)|^2\phi(x,t) + W\delta(x)\phi(x,t). \quad (1)$$

$\phi(x,t)$  denotes here the macroscopic wave function of a system of identical bosons of mass  $m$  evolving in position space and continuous time. Before setting the mapping, we rescale this equation in order to extract the important dimensionless parameters of the superfluid flow. We look for a stationary solution of the form  $\phi(x,t) = \exp(-i\mu t/\hbar)\psi(x)$  with the following boundary condition

$$\psi(x) \Big|_{|x|\rightarrow+\infty} \rightarrow \sqrt{n_0} e^{imv_0x/\hbar}, \quad (2)$$

which describes a solution with asymptotic density  $n_0$  and velocity  $v_0$ . This boundary condition imposes

$$\mu = gn_0 + \frac{1}{2}mv_0^2. \quad (3)$$

We introduce the sound velocity and the healing length according to the standard formulae [1]

$$mc^2 = gn_0, \quad \xi = \frac{\hbar}{\sqrt{mgn_0}} = \frac{\hbar}{mc} \quad (4)$$

and use the rescaled variables  $z = x/\xi$  and  $\tilde{\psi} = \psi/\sqrt{n_0}$  which yields the following universal equation

$$\left[1 + \frac{1}{2}\mathcal{M}^2\right]\tilde{\psi}(z) = -\frac{1}{2}\tilde{\psi}_{zz} + \Lambda\delta(z)\tilde{\psi} + |\tilde{\psi}(z)|^2\tilde{\psi}(z) \quad (5)$$

which depends on two dimensionless parameters, the Mach number and the effective impurity strength

$$\mathcal{M} = \frac{v_0}{c}, \quad \Lambda = \frac{m}{\hbar^2}W\xi. \quad (6)$$

The existence of such a superfluid solution is therefore governed by a precise set of parameters  $\mathcal{M}$  and  $\Lambda$  as demonstrated in Refs. [2, 3] for instance.

We now compare the evolution operator associated to the Gross Pitaevskii equation (1) to the one of our model presented in the main text in the limit of small  $x$  where the cosine can be linearised. This steps allows to map a lattice model to a continuous one. In addition, we take the limit of a vanishing kicking period that makes the dynamics conservative. Then, the formal mapping presented in

Gross-Pitaevskii	Kicked rotor ( $\hbar = 1, n_0 = 1$ )
$p$	$x$
$m$	$1/K$
$g$	$g$
$W$	$W$
$v_0$	$Kx_0$
$c = \sqrt{gn_0/m}$	$c = \sqrt{Kg}$
$\xi = \hbar/mc$	$\xi = \sqrt{K/g}$
$\mathcal{M} = v_0/c$	$\mathcal{M} = Kx_0/c$
$\Lambda = \frac{m}{\hbar^2} W\xi$	$\Lambda = \frac{W\xi}{K}$

Table 1: Dictionary of the mapping between the conservative Gross-Pitaevskii equation and the non-linear kicked rotor at low energy.

Table 1 immediately follows this considerations. Surprisingly, we show in the main text that superfluid features persists in the Floquet dynamics which represents one of the main results of our work.

We note especially that, besides the sound velocity and the healing length, the Mach number and the effective impurity strength also depends on the effective mass  $m = 1/K$ . To complement our results on the critical velocity in the periodically kicked system presented in Fig. 2 of the main text, we here present additional results with different kick strength  $K$  in Fig. 1. We observe an excellent agreement between our numerically determined critical velocities and the analytical prediction for several kick strength  $K$  with  $W\xi/K = \Lambda_c(Kx_c/c)$  where

$$\Lambda_c(z) = \frac{\sqrt{2}}{4z} \sqrt{-8z^4 - 20z^2 + 1 + (1 + 8z^2)^{3/2}}. \quad (7)$$

**Bogoliubov expansion in the periodically kicked system without impurities.** – In the main text, we have discussed that similar quantities to the sound velocity and healing length  $c = \sqrt{gK}, \xi = \sqrt{K/g}$  can be defined in the periodically kicked system when looking at low-energy excitations on top of a stationary solution. Here we provide more details about the derivation and give numerical verification of our results on the linear dispersion and the dynamical instability.

Let us consider a clean superfluid under periodic driving with  $W = 0$ . Our periodically driven system is then described by the following nonlinear time-dependent Schrödinger equation,

$$i\partial_t \psi(p, t) = (-K \cos(x) \sum_m \delta(t - m) + g|\psi(p, t)|^2) \psi(p, t). \quad (8)$$

Conventionally, we may assume an initial state forms a condensate and its dynamics is given by the time evolution above as a good description. In our case, we can check that any plane wave in momentum space given by  $\psi^0(p, t) = \frac{1}{\sqrt{N}} e^{-i\phi(t)} e^{-ipx_0}$  is stationary under the time evolution of Eq. 8 with  $\dot{\phi}(t) = -K \cos(x_0) \sum_m \delta(t - m) + g$ . Given

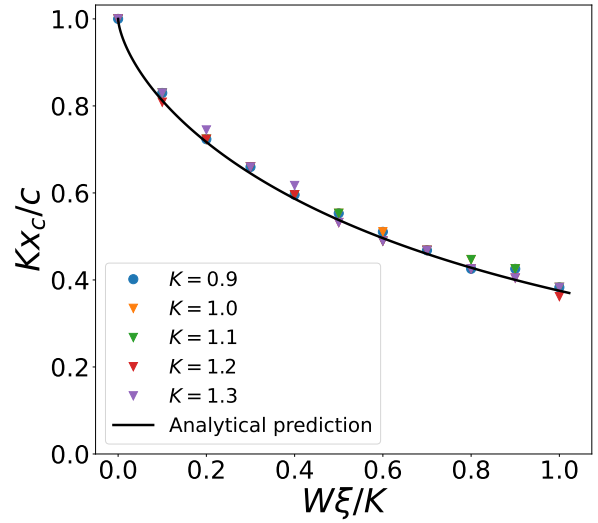


Fig. 1: Numerically determined critical velocity under different kick strength. Analytical prediction is given by  $W\xi/K = \Lambda_c(Kx_c/c)$  with Eq. 7. Other parameters are  $g = 0.1$  and  $N = 1024$ .

this time-dependent solution, the basic idea of the Bogoliubov expansion is to consider a small perturbation on top of it. There are several ways to parameterise the perturbation, and we choose the following form for technical convenience [4],  $\psi(p, t) = \psi^0(p, t)(1 + \delta\psi(p, t))$ . Using this parametrisation and after linearising the nonlinear equation Eq. 8, we can obtain the time-dependent Bogoliubov-de Gennes equations for the perturbation, which take the general form,

$$i\partial_t \begin{pmatrix} \delta\psi(p, t) \\ \delta\psi^*(p, t) \end{pmatrix} = \mathcal{L}(p, t) \begin{pmatrix} \delta\psi(p, t) \\ \delta\psi^*(p, t) \end{pmatrix}, \quad (9)$$

where

$$\mathcal{L}(p, t) = \begin{pmatrix} \mathcal{F}(p, t) & g|\psi^0(p)|^2 \\ -g|\psi^0(p)|^2 & -\mathcal{F}(p, t)^* \end{pmatrix}$$

with  $\mathcal{F}(p, t) = -K \cos(x_0) \sum_m \delta(t - m) + 2g - \frac{i\partial_t \psi^0(p, t)}{\psi^0(p, t)}$  and  $\frac{i\partial_t \psi^0(p, t)}{\psi^0(p, t)} = \dot{\phi}(t)$ . Next, we decompose the perturbation into different Fourier modes labeled by  $\theta$ ,

$$\delta\psi(p, t) = u(\theta, t) e^{ip\theta} + v^*(\theta, t) e^{-ip\theta} \quad (10)$$

with  $\theta$  ranges from  $-\pi$  to  $\pi$ . Substituting the decomposition into Eq. 9, we have

$$i\partial_t \begin{pmatrix} u(\theta, t) \\ v(\theta, t) \end{pmatrix} = \mathcal{M}(\theta, t) \begin{pmatrix} u(\theta, t) \\ v(\theta, t) \end{pmatrix}, \quad (11)$$

where

$$\mathcal{M}(\theta, t) = \begin{pmatrix} \mathcal{Y}(\theta, t) & g \\ -g & -\mathcal{Y}(\theta, t)^* \end{pmatrix}$$

and  $\mathcal{Y}(\theta, t) = -(K \cos(\theta) - K \cos(x_0)) \sum_m \delta(t - m) + g$ , which is the equation presented in the main text.

We can time evolve the Bogoliubov equations of motion in Eq. 11 over one period, and this gives us the one-period evolution operator, i.e. the Floquet operator,

$$\begin{aligned} U(\theta) &= \mathcal{T} e^{-i \int_0^1 dt \mathcal{M}(\theta, t)} \\ &= e^{-i \begin{pmatrix} \lambda & 0 \\ 0 & -\lambda \end{pmatrix}} e^{-i \begin{pmatrix} g & g \\ -g & -g \end{pmatrix}} \\ &= \begin{pmatrix} e^{-i\lambda(1-ig)} & -ie^{i\lambda}g \\ ie^{-i\lambda}g & e^{i\lambda}(1+ig) \end{pmatrix} \end{aligned} \quad (12)$$

with  $\mathcal{T}$  denoting the time order operator and  $\lambda = -K \cos(\theta) + K \cos(x_0)$ . From the second line to the third

line, we used  $e^{-i \begin{pmatrix} g & g \\ -g & -g \end{pmatrix}} = 1 - i \begin{pmatrix} g & g \\ -g & -g \end{pmatrix}$ , since the square of the matrix in the exponent is zero. From the perspective of dynamical instability, we can extract the "Lyapunov" exponents by solving the eigenvalue equation

$$U(\theta)|\phi(\theta)\rangle = e^{i\omega(\theta)}|\phi(\theta)\rangle \quad (13)$$

with the eigenvalue given by

$$e^{i\omega(\theta)} = (\cos \lambda - g \sin \lambda) \pm \sqrt{g^2 - (g \cos \lambda + \sin \lambda)^2}. \quad (14)$$

The appearance of negative imaginary parts in  $\omega(\theta)$  indicates a dynamical instability, i.e. an exponential growth of the associated mode  $\theta$  at the rate  $s_\theta = -\text{Im}\omega(\theta)$ . Considering different kick strength  $K$  with a fixed nonlinearity strength  $g$ , we find that the initial solution with  $x_0 = 0$  is unstable against perturbations when  $K + g > \pi/2$ , as presented in Fig. 2(b). This instability will soon dominate the dynamics as long as there is a nonvanishing perturbation on the unstable modes. This underlies the reason for our consideration of the kick strength  $K + g < \pi/2$ , for example  $K = 1$  or  $K = 1.3$  with  $g = 0.1$  in our main text. It has also been shown that in the prethermal plateau realised by such setting, the thermalisation time is shorter for larger kick strength [5]. It is important that we can clearly observe the thermalisation time for the prethermal phase within our numerical simulation time. Otherwise, it is difficult to distinguish whether the stability of the superfluid is due to the inaccessibly long prethermal plateau or its robustness to Floquet heating.

When the quasi-energy  $\omega(\theta)$  (defined modulo  $\Omega = 2\pi/T$ ) is real, its associated mode is norm conserving and stationary for the periodically driven system. These states are similar to the eigenstates of a time-independent Hamiltonian, except that they are only stationary if we focus on the time points of integer multiples of the periods. To illustrate this point better, we can also construct an operator from  $U(\theta)$  restricted in the first Brillouin zone of the quasi-energy, i.e. the Floquet Hamiltonian,

$$H_F(\theta) = -i \ln U(\theta) \quad (15)$$

to effectively describe the dynamics in the periodically driven system. Generally, this operator can be highly

non-local since the evolution operators during one period do not commute. There are several methods to approximate  $H_F(\theta)$  in the high driving frequency regime, e.g. [6, 7], while here we employ the Baker-Campbell-Hausdorff (BCH) formula [8] to approximate  $H_F(\theta)$ . Our focus here is the dynamics of the low-energy excitation for the initial state with  $x_0 = 0$  under weak nonlinear strength, i.e.  $g$  and  $\theta$  are small. Using  $\cos(\theta) \approx 1 - \theta^2/2$ , we thus assume  $g, \lambda \ll 1$  in the following approximation.

The BCH formula is the solution for the operator  $Z$  to the equation

$$e^X e^Y = e^Z \quad (16)$$

for possibly noncommutative operators  $X$  and  $Y$ . We may write  $Z$  as a formal series in  $X$  and  $Y$  and iterated commutators thereof, and the first few terms of this series are:

$$\begin{aligned} Z &= X + Y + \frac{1}{2}[X, Y] \\ &+ \frac{1}{12}[X, [X, Y]] - \frac{1}{12}[Y, [X, Y]] + \dots \end{aligned} \quad (17)$$

where  $\dots$  indicates terms involving higher commutators of  $X$  and  $Y$ . Note that the series is not necessarily convergent for generic cases. Noting that in our model

$$X = -i \begin{pmatrix} \lambda & 0 \\ 0 & -\lambda \end{pmatrix}; Y = -i \begin{pmatrix} g & g \\ -g & -g \end{pmatrix} \quad (18)$$

we can write the first few terms for the effective Floquet Hamiltonian,

$$\begin{aligned} H_F(\theta) &= H_F^{(1)}(\theta) + H_F^{(2)}(\theta) + \dots \\ &= \begin{pmatrix} \lambda + g & g \\ -g & -\lambda - g \end{pmatrix} - i \begin{pmatrix} 0 & g\lambda \\ g\lambda & 0 \end{pmatrix} + O(\epsilon) \end{aligned} \quad (19)$$

where  $\epsilon$  denotes higher order terms in  $g, \lambda$ . We presented the effective quasi-energy by considering only up to the first term  $H_F^{(1)}(\theta)$  in the main text for simplicity. Here the quasi-energy up to second order in  $g, \lambda$  is presented,

$$\omega_{\pm}^{(1)}(\theta) + \omega_{\pm}^{(2)}(\theta) = \pm \sqrt{\frac{K\theta^2}{2} \left( (1-g^2)\frac{K\theta^2}{2} + 2g \right)}. \quad (20)$$

We observe that the linear dispersion still exists for low-energy excitations. Alternatively, we may resort to numerically diagonalise Eq. 13 to obtain the quasi-energy  $\omega_+(\theta)$  to all orders or take derivative of  $\omega_+(\theta)$  in Eq. 14 with respect to  $\theta$  for small  $\theta$ . We plot  $\omega(\theta)$  vs.  $\theta$  in Fig. 2(a) and a linear dispersion relation is clearly observed for small  $\theta$  up to  $1/\xi$  with velocity  $c = \sqrt{gK}$  and healing length  $\xi = \sqrt{K/g}$ . Note that the dynamical instability for large kick strength  $K$  does not appear in the approximation presented above, since it may be in a regime where the assumption  $\lambda \ll 1$  does not hold and contributed by higher order terms in the series expansion. As demonstrated in Fig. 2(b), the instability indeed occurs at  $\theta \approx \pi$ , i.e.  $\lambda \approx -2K$ .

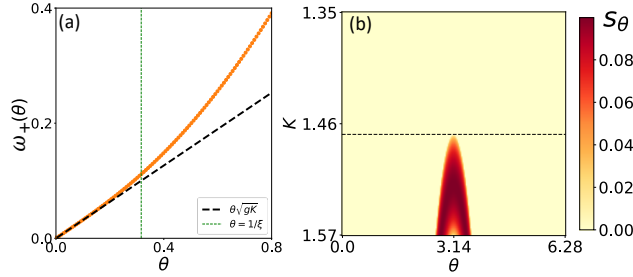


Fig. 2: (a) Quasi-energy of the Floquet operator  $\omega(\theta)$  (positive branch) vs.  $\theta$  shown in the orange line. The linear dispersion with velocity  $c = \sqrt{gK}$  is indicated by the black dashed line and the vertical green dashed lines is at  $1/\xi$  with  $\xi = \sqrt{K/g}$ . Parameters used are  $g = 0.1$  and  $K = 1$ . (b) Dynamical instability diagram showing the instability rate  $s_\theta$  as a function of the kicking strength and the mode  $\theta$ . Instability occurs at  $\theta = \pi$  when  $K + g \approx \pi/2$ . The black dashed line denotes  $K = \pi/2 - g$ .

**Details of the derivation of the effective impurity strength in the disordered kicked rotor.** – We explain here the renormalisation procedure that we use in order to replace the full disorder potential with a single impurity using screening arguments and extreme value statistics. We first construct a coarse grained potential by summing up all the impurities in a window of size  $\alpha\xi$ , with  $\alpha$  a parameter of order unity that will be fixed by fitting a single set of data. Starting from  $N$  impurities of strength  $u_i \in [-\frac{W}{2}, \frac{W}{2}]$  with uniform distribution, we have  $\langle u \rangle = 0$ ,  $\langle u_i u_j \rangle = \frac{W^2}{12} \delta_{ij}$  and define a renormalised potential

$$\tilde{u}_j = \sum_{\text{box } j} u_i. \quad (21)$$

Each box contains  $M_\alpha = \alpha\xi/\Delta p$  impurities, where  $\Delta p$  is the discretisation in  $p$  space ( $\Delta p = 1$  in our work) and the total number of box is  $B = N/M_\alpha$ . The idea is then to look for the dominant contribution that comes from the maximum of this new disorder  $\tilde{u}_m = \max\{\tilde{u}_j\}$ . Then, everything boils down to a problem of extreme value statistics.

We first look at the statistics of  $\tilde{u}_j$ . Note that  $\tilde{u}_j$  is a sum of independent random variables with the same uniform distribution. It rapidly converges ( $M_\alpha \geq 5$  is enough for our purpose) to a normal distribution with zero mean and variance  $\sigma^2 = M_\alpha \frac{W^2}{12}$ . The statistics of  $\tilde{u}_m = \max\{\tilde{u}_j\}$  is a standard problem of extreme value statistics, and we briefly explain it here. A simple question to answer is to find the probability for the maximum to be smaller than a given value  $y$  (this is the cumulative distribution of the maximum). In order for the maximum being smaller than  $y$ , all the  $\tilde{u}_j$  have to be smaller than  $y$ . Since the  $B$  random variables are independent, the result is just the product of their respective cumulative distributions  $F(y)$ . We therefore end up with a simple equation for the cumulative distribution  $\mathcal{F}_B$  of  $\tilde{u}_m$ ,

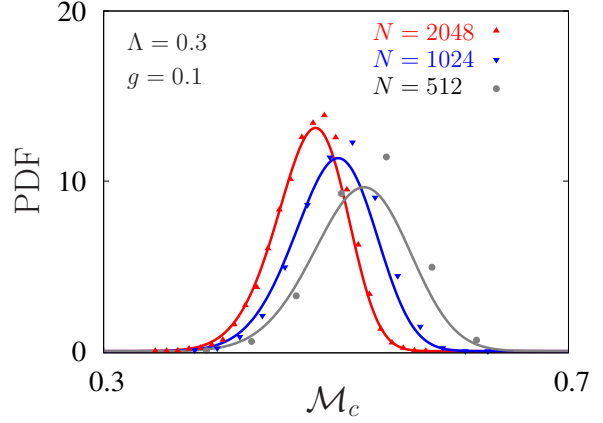


Fig. 3: Probability distribution of the critical mach number  $\mathcal{M}_c = Kx_c/c$  for different system size at constant disorder strength  $\Lambda = W\xi/K = 0.3$ ,  $K = 1$  and  $g = 0.1$ . Full curves are analytical predictions extracted from Eq. (25) and symbols are numerical simulations of the kicked rotor as explained in the main text.

$$\mathcal{F}_B(\tilde{u}_m) = F(\tilde{u}_m)^B. \quad (22)$$

Note that for a Gaussian variable  $z$  with distribution  $p(z) = \exp[-z^2/2\sigma^2]/\sqrt{2\pi\sigma^2}$ , we have

$$F(z) = \int_{-\infty}^z dy p(y) = \frac{1 + \operatorname{erf}\left(\frac{z}{\sqrt{2}\sigma}\right)}{2}. \quad (23)$$

We now use the crude approximation of replacing the full complexity of the microscopic disorder with a single-site impurity of effective strength  $\tilde{u}_m$  and apply the criterion (Eq. 7) to compute the critical  $x_0$ , namely

$$\frac{\tilde{u}_m \xi}{K} = \Lambda_c(Kx_c/c). \quad (24)$$

This relation being bijective we finally obtain the statistical distribution of  $x_c$  through the following relation between the cumulative distributions

$$\Phi_N(z) = 1 - \mathcal{F}_B(\tilde{u}_m \xi / K = \Lambda_c(z)), \quad (25)$$

with  $z = Kx_c/c$  which yields, together with the previous definition, to the equation of the main text. This simple expression contains however nontrivial scaling properties of  $x_c$  with respect to the system size  $N$ , the disorder strength  $W$ , the kick strength  $K$  and the interaction parameter  $g$  via  $c$  and  $\xi$ . Finally, the parameter  $\alpha$  is determined by fitting the theory to a single set of data. We obtained  $\alpha = 2.78$  which is indeed a parameter of order unity.

In addition to the data shown in the main text we demonstrate in this appendix that the scaling of the critical velocity  $x_c$  with respect to the system size is also well described by this model as shown on Figure 3. As the system size is increased, the distribution is shifted to lower

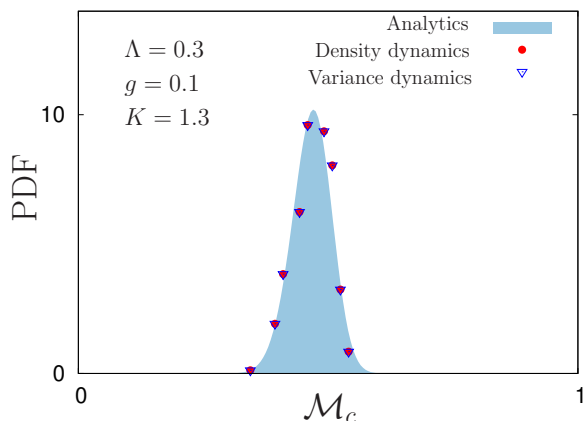


Fig. 4: Probability distribution of the critical Mach number  $\mathcal{M}_c = Kx_c/c$  determined from both the density dynamics and the variance dynamics at constant disorder strength  $\Lambda = W\xi/K = 0.3$ ,  $K = 1.3$  and  $g = 0.1$ . The blue filled curve is the analytical prediction and symbols are numerical results.

$x_0$ . This can be easily understood by the fact that the larger the number of box, the higher the probability to find a large  $\tilde{u}_j$ . Note however, that the Gaussian approximation for  $\tilde{u}_j$  predicts that the critical velocity  $x_c$  vanishes in the thermodynamic limit. This is actually an artefact of this approximation since  $\tilde{u}_j$  is bounded by  $M_\alpha W/2$ . This pathology can be corrected by taking the true distribution of  $\tilde{u}_j$  that can be exactly computed. However, we choose to use the Gaussian approximation in order to avoid cumbersome expressions that are irrelevant in general.

Last, in Fig. 4 we present additional results on the distribution of the critical velocity separating a finite thermalisation time and an "infinite" one for the disordered periodically kicked rotor. Note that "infinite" means we could not observe the thermalisation up to the longest time in our numerical simulation  $10^7$  periods for  $x_0$  slightly below the critical value, much longer than the longest finite thermalisation time  $\sim 10^6$  observed for  $x_0$  slightly above the critical value. We find an excellent agreement between the distribution obtained from the density dynamics and that of the variance dynamics. This confirms again that the superfluid phase we reported in the weakly disordered kicked rotor is robust to heating when  $K + g < \pi/2$ .

## REFERENCES

- [1] PETHICK C. J. and SMITH H., *Bose-Einstein condensation in dilute gases* (Cambridge university press) 2008.
- [2] HAKIM V., *Phys. Rev. E*, **55** (1997) 2835.
- [3] LEOEUF P. and PAVLOFF N., *Phys. Rev. A*, **64** (2001) 033602.
- [4] BUKOV M., GOPALAKRISHNAN S., KNAP M. and DEMLER E., *Phys. Rev. Lett.*, **115** (2015) 205301.
- [5] HALDAR P., MU S., GEORGEOT B., GONG J., MINIATURA C. and LEMARIÉ G., *arXiv e-prints*, (2021)

arXiv:2109.14347.

- [6] GOLDMAN N. and DALIBARD J., *Phys. Rev. X*, **4** (2014) 031027.
- [7] BUKOV M., D'ALESSIO L. and POLKOVNIKOV A., *Advances in Physics*, **64** (2015) 139.
- [8] ACHILLES R. and BONFIGLIOLI A., *Archive for History of Exact Sciences*, **66** (2012) 295.